Numerical Simulation of Tritium Behavior under a Postulated Accident Condition for CFETR TEP System

Authors: Wang, Haixia, Fu, Xuwei, Liu, Weiping, Li, Taosheng, Yu, Jie, Wang, Haixia

Date: 2023-06-09T00:00:00+00:00

Abstract

The China Fusion Engineering Test Reactor (CFETR) represents China's independently designed next-generation fusion reactor project currently under development. Tritium confinement systems in CFETR ensure that radiation levels remain below safety limits during tritium handling and operation within the fuel cycle system. Our tritium technology team is responsible for investigating tritium transport behavior in the CFETR tritium safety confinement system under China's National Key R&D Program launched in 2017, and we are conducting safety analyses of the CFETR tritium plant using CFD software. This paper examines tritium migration and removal behavior under a postulated accident condition in the Tokamak Exhaust Processing (TEP) system of CFETR. Quantitative results are presented for tritium transport behavior throughout the entire accident sequence—including tritium release, alarm activation, isolation, and removal—in both the process room and glove box. These findings support detailed design and engineering demonstration research for the CFETR tritium plant.

Full Text

Preamble

Numerical Simulation of Tritium Behavior under a Postulated Accident Condition for CFETR TEP System

Haixia WANG*, Xuewei FU, Weiping LIU, Taosheng LI & Jie YU
Institute of Nuclear Energy Safety Technology, Hefei Institutes of Physical Science, Chinese Academy of Sciences, Hefei 230031, China

*Corresponding author: Haixia WANG (E-mail: haixia.wang@inest.cas.cn)

Abstract

The China Fusion Engineering Test Reactor (CFETR) represents China's independently designed next-generation fusion reactor project currently under development. Tritium confinement systems in CFETR ensure that radiation levels remain below safety limits during tritium handling and operation within the fuel cycle system. Our tritium technology team is responsible for investigating tritium transport behavior in the CFETR tritium safety confinement system under China's National Key R&D Program launched in 2017, and we are conducting safety analyses of the CFETR tritium plant using CFD software. This paper examines tritium migration and removal behavior under a postulated accident condition in the Tokamak Exhaust Processing (TEP) system of CFETR. Quantitative results are presented for tritium transport behavior throughout the entire accident sequence—including tritium release, alarm activation, isolation, and removal—in both the process room and glove box. These findings support detailed design and engineering demonstration research for the CFETR tritium plant.

Key words: China Fusion Engineering Test Reactor (CFETR), Tokamak Exhaust Processing (TEP) system, Numerical simulation, Tritium transport behavior, Tritium confinement system, Accident condition

Introduction

For CFETR, which is designed with high safety and acceptability standards, tritium safety represents one of the most critical issues. Tritium must be effectively controlled to prevent excessive release into the atmosphere and to protect workers from exposure. According to CFETR's tritium safety principle, tritium should be handled within multiple confinement barriers monitored by detritiation systems—a concept that has been successfully implemented in tritium facilities worldwide [1-5].

Tritium is both expensive and scarce, and experimental studies involving tritium are costly and challenging. Consequently, numerical simulation has become an essential tool for investigating tritium leakage and diffusion patterns. Previous studies have demonstrated that three-dimensional flow analysis codes can reproduce and simulate tritium migration and removal behavior with remarkable accuracy [6-13]. Recognizing the importance of tritium safety for CFETR, the Government of the People's Republic of China launched the National Key R&D Program in 2017 to conduct "Research on digital technology of CFETR tritium plant." As a participating team in this program, our tritium technology group is responsible for three-dimensional studies of tritium transport behavior in the CFETR tritium safety confinement system. If the first physical barrier fails, tritium will leak into the second barrier, such as a glove box. Our prior research has reported on postulated pipeline rupture events in the Tokamak Exhaust Processing (TEP) System of CFETR, using finite element software COMSOL to model tritium migration and removal behavior within the glove box [14-16].

A room or building where personnel work serves as the final tritium confinement barrier to the environment. However, few studies have investigated tritium behavior following failure of more than one barrier. The primary objectives of our ongoing research are: (1) to investigate tritium mixing and migration in both the process room and glove box under conditions of double physical barrier failure, and (2) to evaluate the cleanup performance of the detritiation system in the process room. This paper discusses both initial tritium behavior immediately after release and removal behavior during ventilation system operation. The results support ongoing detailed design and engineering demonstration research for the CFETR tritium plant.

1.1 Brief Introduction to CFETR TEP System

The TEP system is one of the most critical components in CFETR's inner fuel cycle, with its main design goal being the treatment of plasma exhaust gas from the vacuum vessel and the recovery of most tritium contained in the gas. Similar to ITER's TEP system [17], CFETR's TEP system employs a three-stage process to treat plasma exhaust gas: front-end processing, impurity processing, and final cleanup processing [18]. Equipment for the front-end processing system is housed in a dedicated glove box served by a Glove box Detritiation System (GDS), while the other two systems share a second glove box with another GDS. Before environmental release, the remaining waste gas is temporarily stored in a decay tank. Power distribution cabinets (PDCs) are specially installed to supply electricity. All these subsystems and components of the TEP system are located within a dedicated process room [FIGURE:1].

During normal operation, the process room is maintained at negative pressure (-100 Pa) by the HVAC (heating, ventilation, and air conditioning) system. If airborne contamination is detected, control actions are implemented by the Detritiation Systems (DSs). The ventilation of the affected room is isolated from the HVAC system by the detritiation system, and the following measures are undertaken depending on contamination levels: (a) all personnel are evacuated, (b) the contamination source is identified and isolated, and (c) the detritiation system is activated and maintains depression in the affected room or area through a pressure controller and flow damper.

1.2 Description of Postulated Accident

The postulated initiating event is the instantaneous failure of a tritium process line in the front-end processing system at maximum design flow rate. Because the process line pressure exceeds that of the glove box, process gas is released into the glove box, causing tritium concentration to increase rapidly. If the glove box system also fails, tritium sprays into the process room through the breach, resulting in rapid elevation of tritium concentration in the process room.

According to the latest CFETR design, a tritium concentration in the process room equal to or exceeding 1 DAC (3.5×10^5 Bq/m^3, alarm set point) triggers a

contamination alarm, initiating operator evacuation procedures. If the tritium release exceeds the threshold of 1×10^8 Bq/m^3 (isolation set point), the failed tritium process line is isolated according to control system instructions, and the DS automatically isolates the affected sector from the HVAC system while activating detritiation and depression functions. The DS purges the contaminated process room with air to decontaminate the atmosphere, with a design flow rate of 9000 m^3/h. All these parameters (alarm set point, isolation set point, and design flow rate) are provided by the CFETR tritium plant designer. The tritium leak route is: process line → glove box → process room → DS → environment, and the accident time sequence is summarized in Table 1 .

Notably, a time interval exists between detection of exceeded tritium concentration and the isolation of the process line and initiation of the DS. This delay time is designed to be 300 s. Consequently, during this 300-s delay, tritium concentration continues to increase in both the glove box and process room until the DS begins purging.

2.1 Governing Equations

The aforementioned accident involves a three-level confinement system: the first barrier is the TEP process pipeline (failed), the second barrier is the glove box system (failed), and the third barrier is the process room. The transport of leaked tritium in the process room and glove box is essentially a mass transfer problem of fluid in motion, governed by the fundamental equations of fluid dynamics: conservation of mass, momentum, and energy.

All released tritium is assumed to be in the form of T_2. Tritium adsorption, desorption, and isotope exchange reactions are not considered in this work because humidity and oxygen content in the glove box and room are designed to be low. Temperature is maintained constant at 295 K during the accident, and no effective heat source is present in the process room, making energy transport considerations unnecessary. The gas velocity in the glove box and process room is lower than the local sound velocity, with Mach number (Ma) well below 0.3 in over 90% of the space. Therefore, density changes in this low-velocity gas flow can generally be ignored, meaning the gas can be treated as incompressible.

The governing equations for the working gas flow simulation are expressed as Eq.1 and Eq.2. The Reynolds-Averaged Navier-Stokes (RANS) and k- turbulence model [19] equations are given as Eq.3-Eq.6.

$$0\nabla \cdot \mathbf{u} = 21p\mu t\rho \mathbf{uufu}\partial + \cdot\nabla = -\nabla + \nabla\partial$$

where velocity vector $\mathbf{u}$ and pressure p are the variables to be determined in this study. (kg/m^3) represents density and (Pa · s) represents dynamic viscosity. $\mathbf{f}$ (N) represents body force. k (m^2/s^2) and (m^2/s^3) represent turbulent kinetic energy and turbulent kinetic energy dissipation rate, respectively. The turbulence model coefficients are listed in Table 2 .

During tritium transport, fluid component transport processes occur because leaked tritium mixes with nitrogen in the glove box and air in the process room. COMSOL predicts the local mass fraction of each component by solving the component transport equation. Tritium leakage during the entire accident is predicted to be less than 10% of the glove box volume, and this ratio is even smaller for the process room. Therefore, treating tritium as a dilute substance relative to the background gas (nitrogen or air) is reasonable. The tritium transport process is described by convection and diffusion equations, Eq.7 and Eq.8, respectively.

$$\frac{\partial c_i}{\partial t} + \mathbf{u} \cdot \nabla c_i + \nabla \cdot \mathbf{J}_i = R_i$$

where c ($\mathrm{Bq/m^3}$) represents concentration, the variable to be determined in this study. $\mathbf{J}$ ($\mathrm{Bq/m^2/s}$) represents the diffusion flux vector. R ($\mathrm{Bq/m^3/s}$) represents the reaction term, which is set to 0. D ($\mathrm{m^2/s}$) represents the diffusion coefficient, with values obtained from literature [8]: 5.65×10^{-6} $\mathrm{m^2/s}$ for tritium in nitrogen and 7.41×10^{-6} $\mathrm{m^2/s}$ for tritium in air.

Notably, in the process room, only tritium transport in air is considered, ignoring nitrogen leaking from the glove box into the process room. This assumption is made because: (a) tritium is the research focus, (b) there is a substantial volume difference between the glove box (2.62 $\mathrm{m^3}$) and the room (242.09 $\mathrm{m^3}$), and (c) 80% of air is nitrogen; thus, even if all nitrogen from the glove box entered the process room, it would have minimal influence on tritium transport in air. In other words, only one gas species is considered in Eq.7 and Eq.8, and the subscript i refers only to tritium.

2.2 Geometric Model

Based on information from the China Academy of Engineering Physics (responsible for CFETR tritium plant design), a three-dimensional geometric model was constructed using the geometric kernel of COMSOL [FIGURE:2]. The interior of the TEP process room is a complete rectangular parallelepiped (10.83 m × 6 m × 4 m), filled with air and maintained at a negative pressure of 100 Pa below atmospheric pressure. Within the process room are three glove boxes serving: (1) front-end processing, (2) impurity processing and final cleanup processing, and (3) the gamma decay tank. Additionally, two PDCs (PDC-1 and PDC-2) stand against a wall.

Two simulation domains are defined in this study: (1) Simulation Domain 1 (SD-1) is the entire 3.82 m × 0.667 m × 1.2 m rectangular volume in GB-1, filled with nitrogen and maintained at a negative pressure of 200 Pa below atmospheric pressure. This domain contains one cylindrical buffer tank (Φ0.3 m × 0.55 m) and four cylindrical permeators (Φ0.4 m × 0.8 m), all placed vertically on the ground. Tritium from the TEP process line injects into the glove box through the assumed leak hole (Hole-1), which is set at the top of

the second permeator with Φ0.04 m in the accident scenario. (2) Simulation Domain 2 (SD-2) is the process room space. Tritium diffuses from the glove box into the process room through Hole-2 (Φ0.04 m) located on the front surface of GB-1 in the accident. The coordinates of Hole-2 are set at (4.178, 1.500, 1.500) based on analysis of probable glove damage positions due to long-term service. The DS in the process room is assumed to have supply and exhaust ducts in the left and right walls, operating in once-through mode with a fixed fluid flow rate.

Nine monitors (GB-M1 to GB-M9) are positioned in SD-1 for tritium concentration monitoring, and fifteen monitors (PR-M1 to PR-M15) are positioned in SD-2. Table 3 provides the coordinates of tritium leak holes, tritium monitors, and the center points of supply and exhaust ducts in the process room.

The working gas properties for nitrogen in the glove box and air in the process room use parameters from the COMSOL material library. The software automatically sets nitrogen density (1.15 kg/m^3) and viscosity coefficient (1.75 $\times$ 10^{-5} $Pa \cdot s$) based on the glove box environment (295 K, 1 atm - 200 Pa = 101125 Pa). Similarly, air density (1.20 kg/m^3) and viscosity coefficient (1.82 $\times$ 10^{-5} $Pa \cdot s$) are automatically set based on the process room environment (295 K, 1 atm - 100 Pa = 101225 Pa). Tritium diffusion coefficients are obtained from literature [8] and were introduced in Section 2.1.

2.3 Boundary Conditions and Initial Values

During the tritium release stage of the accident, the boundary condition at Hole-1 is set as a velocity boundary with magnitude given by Eq.9 [20]:

$$v = \sqrt{\frac{2k}{k-1} RT \left[1 - \left(\frac{P_2}{P_1} \right)^{\frac{k-1}{k}} \right]}$$

where v represents leakage velocity ($m \cdot s^{-1}$), k represents the gas adiabatic index (1.4), R represents the gas constant (8.314), T represents temperature (300 K), P_1 represents pressure in the tritium process line (0.25 MPa), and P_2 represents pressure in the glove box (1 atm - 200 Pa). Based on these values and Eq.9, the breach velocity is approximately 63.4 $m \cdot s^{-1}$.

Walls shared by SD-1 and SD-2 are set as interior walls and thin impermeable barriers. Other wall boundaries are set to no-slip wall conditions. Because the DS is not activated during the release stage, the supply vent boundary is set as a wall boundary, while the exhaust vent boundary condition is a pressure boundary with relative pressure of -100 Pa. Initial tritium concentrations in both SD-1 and SD-2 are set to 0 Bq/m^3.

During the tritium removal stage, because tritium leakage from the holes has ceased, the boundary condition at Hole-1 is reset to a wall boundary. The supply vent boundary condition is reset to a flow rate boundary, with flow rate set to

9000 $m^3 \cdot s^{-1}$ according to DS design. Walls shared by SD-1 (glove box) and SD-2 (process room), including the wall containing Hole-2, remain as interior walls and thin impermeable barriers. The exhaust vent maintains the pressure boundary at a relative pressure of -100 Pa.

3. Results and Discussion

Numerical simulations were performed to investigate tritium transport performance under fixed ambient conditions and leak apertures (and positions). This paper focuses on changes in tritium concentration and removal characteristics in the process room (SD-2), which directly relate to on-site personnel safety and the amount of tritium released to the environment. Tritium behavior in the GB-1 space was also studied to understand the complete tritium transport process, particularly concentration changes in the room. Unless otherwise specified, "glove box" herein refers to SD-1, not the entire GB-1 or the other two glove boxes.

3.1.1 Contours of Tritium Concentration

Using COMSOL's powerful visualization capabilities, Figure 3 [FIGURE:3] presents concentration contour maps to observe the three-dimensional evolution of tritium transport. Approximately 0.01 s after instantaneous failure of the tritium process line, tritium reaches the top of the glove box, with the diffusion shape resembling a flower bud. This "flower" subsequently blooms, with outer petals symmetrically covering the entire y-direction of the glove box top at 0.026 s. As the outer petal tops increase in size and reach Hole-2 at 0.078 s, the symmetry is broken. The "flower" continues blooming, but the outer petal tops are disrupted.

Tritium concentration contours in the process room exhibit similar patterns. As shown in Figure 4 [FIGURE:4], approximately 2.30 s after the accident, the symmetrical outer petal of the tritium "flower" reaches the nearest vertical wall of the process room. As the outer petal tops increase in size along the wall, they symmetrically reach the bottom of the wall at 23.67 s. The "flower" then continues moving along the wall and floor, and as dispersion proceeds, vortex phenomena become more pronounced. As illustrated in Figures 3 and 4, tritium migrates more rapidly along walls than through open space, facilitating understanding of the petal movement.

3.1.2 Slices of Tritium Concentration

Figures 5 and 6 show tritium concentration slices. As depicted in the first image of Figure 5

, at the moment of breach, tritium is rapidly ejected from Hole-1 (in the pipeline) and reaches the top of the glove box within 0.01 s, resembling a burning candle from this perspective. The "smoke" from this "candle" moves approximately

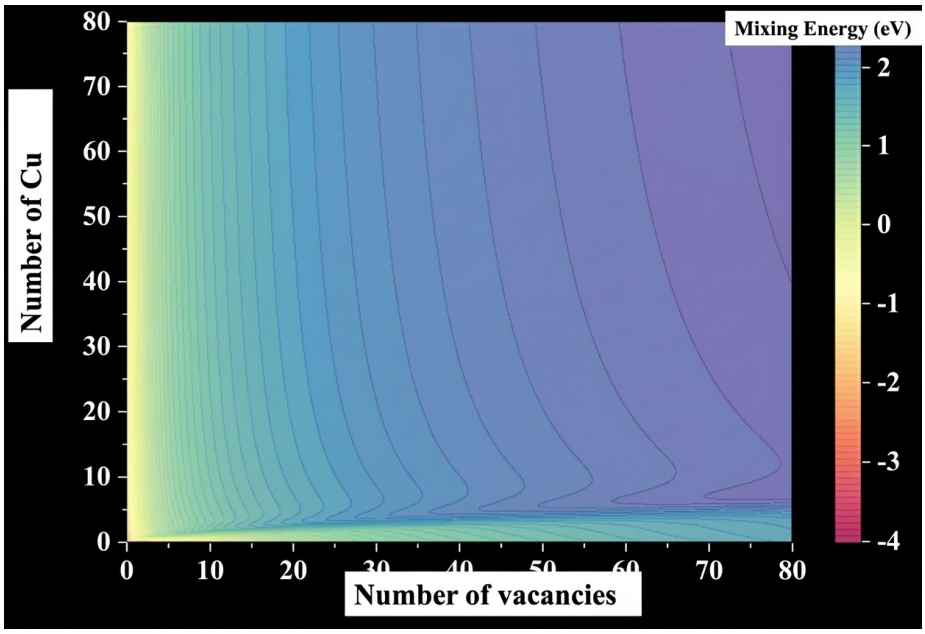

Figure 1: Figure 5

symmetrically to the left and right sides, forming an umbrella-shaped "smoke" distribution beneath the glove box's top wall. As release time increases, tritium concentration rises, and maximum velocity remains observed at the leak hole, specifically along the jet flow centerline. At the end of the tritium release stage (300 s), tritium concentration throughout the glove box reaches 2.36~3.13 $\times$ 10^{15} Bq/m^3.

As shown in Figure 6 [FIGURE:6], tritium in the glove box migrates more rapidly along walls than through space. Tritium escapes from the glove box into the process room via three primary routes: (1) tritium ejected from Hole-1 into the glove box top migrates along the -y direction and then downward into Hole-2; (2) tritium injected into the glove box top migrates along the +y direction and other directions, then downward to the glove box bottom and upward into Hole-2; and (3) under concentration and velocity gradient driving forces, tritium in the glove box space moves into Hole-2.

3.1.3 Concentration at Monitoring Points

Variations in tritium concentration at monitoring points provide quantitative safety-relevant information. Figure 7a [FIGURE:7] shows tritium concentration variations from 0 to 300 s at nine monitoring points in the glove box. Key conclusions from Figure 7a include: (1) All monitoring points exhibit similar concentration trends, with rapid climb from 0 to 1 $\times$ 10^{14}~15 Bq/m^3 during

the first 2.5 s, followed by slow increase. After approximately 60 s, tritium concentration essentially reaches a constant value, forming two groups: 1.63~1.73 $\times$ 10^{15} Bq/m^3 and approximately 2.57~2.63 $\times$ 10^{15} Bq/m^3. (2) Initially, tritium concentration is highest at GB-M6, followed by GB-M5/GB-M7. Within 0.06 s, concentrations at GB-M6 and GB-M5/GB-M7 exceed 10^{10} Bq/m^3. This is understandable because GB-M6 is located directly above Hole-1, and GB-M5/GB-M7 are on walls very close to Hole-1. For GB-M5 and GB-M7, which are spatially symmetric about the pipeline breach, tritium concentration shows essentially uniform steps, with the former being closer to Hole-2 than the latter, resulting in slightly higher concentration during certain periods. A similar phenomenon was observed in [10], where concentrations under open-space conditions were slightly higher than under closed-space conditions because closed boundaries suppress tritium diffusion. (3) GB-M1 and GB-M3, and GB-M2 and GB-M4, are nearly two groups of spatial symmetry points far from Hole-1 and Hole-2, showing uniform variation patterns for each group's symmetric points. GB-M8 and GB-M9 are perfect symmetry points, with concentration change lines almost coinciding. (4) Notably, concentration inversion occurs: in the first 4 s, concentrations at GB-M6 and GB-M5/GB-M7 are higher than at the other six monitoring points, but after 23 s, concentrations at GB-M6 and GB-M5/GB-M7 become significantly lower than at other points. The probable reason is that tritium moves faster along walls than through space. In the first 4 s, more tritium reaches GB-M6 and GB-M5/GB-M7 than escapes to other monitoring points in the process room (see cases at 0.10 s and 1.02 s in Figures 5 and 6). As tritium concentration increases and spatial distribution becomes uniform across the nine monitoring points (see cases at 7.80 s and 20.91 s in Figures 5 and 6), more tritium escapes into the process room along walls after 23 s compared to other monitoring points.

Figure 7b shows tritium concentration variations from 0 to 300 s at fifteen monitoring points in the process room. Key conclusions include: (1) All process room monitoring points show similar concentration trends: rapid climb, slow growth, then approach to a constant value, with different change times at different points. Because the process room space is much larger than the glove box and monitoring points are distributed in representative areas, concentrations at different points show relatively dispersed distribution compared to those in the glove box. A special monitoring point, PR-M11, located between two glove boxes, shows reduced concentration increase due to the complex flow field, appearing "safer" with lower tritium concentration because its location prevents some tritium from flowing through. (2) Throughout the tritium release period, PR-M2 shows the highest concentration, followed by PR-M1, because they lie in the direct path of tritium escaping from Hole-2. Initially, the next highest points are PR-M3, PR-M4, and PR-M5, whose concentrations exceed the alarm setpoint (3×10^5 Bq/m^3) within 1.31 s. Due to faster wall migration, once tritium reaches PR-M5 (on the top wall), which is farther from Hole-2 than PR-M3 and PR-M4, its concentration increases more rapidly than at PR-M3 and PR-M4. PR-M7 (on the wall) and PR-M6, and PR-M10 (on the wall) and PR-

M8, show similar trends as PR-M5 and PR-M3/PR-M4. PR-M12, PR-M13, and PR-M15 are far along the tritium migration route, with concentration increases occurring later. (3) From a safety perspective, the monitoring point with the fastest tritium concentration growth rate should be selected as reference, i.e., PR-M2. T1, T2, and T3 in Table 1 occur within 0.05 s after the accident.

Notably, tritium continues releasing during the 300-s interval between detection of exceeded concentration and process line isolation plus DS activation. Therefore, tritium concentration continues increasing in both glove box and process room. At the end of the tritium release stage (300 s), process room tritium concentration reaches $1.02 \sim 7.05 \times 10^{14}$ Bq/m^3. Subsequently, the DS in the process room begins introducing purge air. The highest concentration range in the process room is approximately 7 times larger than the lowest, with more dispersed concentration distribution than in the glove box ($1.63\sim2.63 \times 10^{15}$ Bq/m^3). This results from the process room's much larger space, scattered monitoring points, and complex obstacles to tritium transport.

3.2 Tritium Removal Stage

During the tritium removal stage, when the DS is activated, clean air gradually enters the process room and disrupts the original tritium distribution pattern established during the release stage. The final tritium concentration distribution from the release stage (Section 3.1) serves as the initial distribution for the removal stage. Zero seconds in Section 3.2 marks the start of the removal stage, coinciding with the end of the release stage.

3.2.1 Slices of Tritium Concentration

As clean air enters the process room, tritium concentration decreases first in areas facing or near the supply vent. As shown in Figure 8 [FIGURE:8], a low-concentration region appears at the bottom right corner at 0.20 s, indicating that clean air travels from the supply duct at x = 0 m to x = 4.178 m (Hole-1) in 0.2 s, and this region maintains the lowest tritium concentration. Tritium concentration continues decreasing as more purge air enters. After 30 s, concentration distributions become similar or identical (particularly after 500 s), except for legend ranges. In other words, a relatively stable tritium concentration distribution forms, establishing a new concentration pattern.

3.2.2 Concentration at Monitoring Points

Figure 9 [FIGURE:9] shows tritium concentrations at monitoring points during the removal stage. Driven by the gradient between SD-1 and SD-2, tritium escapes from the glove box through Hole-2, causing glove box tritium concentration to decrease. After an initial short period (approximately 20 s) of irregular decline, tritium concentrations at all glove box monitoring points become nearly a set of log-linear graphs. Two groups with similar slopes but different concentrations appear: one for GB-M6 and GB-M5/GB-M7, and another for

the remaining monitoring points, identical to the grouping during the release stage.

Tritium in the process room is directly driven out by purge air, while tritium continues escaping from the glove box into the process room through Hole-2. The former process dominates, and Figure 9b shows a decreasing concentration trend. Similar to the glove box, the process room experiences a short period (approximately 30 s) of irregular decline, after which tritium concentrations at all monitoring points become nearly log-linear graphs. The slope relates to tritium removal rate, with steeper slopes indicating faster removal. PR-M2 shows obvious advantages in removal rate because the primary flow direction at this location is along the +x direction, moving toward other spaces or the exhaust vent without back-mixing [FIGURE:10]. PR-M15 shows the lowest removal rate, which is easily understood from the streamlines in Figure 10. At this location, the primary flow is characterized as a "spiral flow," with PR-M15 appearing at the spiral center, preventing most tritium from moving directly to the exhaust vent.

The time required for tritium concentration to fall to the isolation threshold is 1941 s, and the time needed to reach the alarm setpoint is approximately 2667 s (equivalent to T4 in Table 1). The DS continues purging the process room for an extended period. After 3000 s of DS operation, the maximum concentration among process room monitoring points decreases to 2.61×10^4 Bq/m^3. At 3600 s, the maximum concentration decreases to 243.5 Bq/m^3, less than 1/1000 of the alarm setpoint and 1/100 of the detection limit for general tritium air monitors. Notably, if the DS in the room stops working, tritium in the glove box will continue leaking, increasing room concentration. However, 1 hour of continuous purging reduces tritium in the glove box and process room to 1.44×10^3 Bq and 4.70×10^4 Bq, respectively [FIGURE:11]. The ratio of glove box volume to process room volume is ~1/100 (2.6192 m^3/242.09 m^3); thus, even if all residual tritium in the glove box entered the room, the effect on room concentration would be slight.

4 Summary

A numerical model for subsonic jet flow of tritium leakage from the pipeline and glove box was developed using COMSOL software to investigate tritium transport behavior under a postulated accident condition in the CFETR TEP system. This paper focused on tritium concentration and removal characteristics in the process room because they directly relate to on-site personnel safety. Changes in tritium concentration in the glove box were also studied to understand the complete tritium transport process.

(1) Tritium Release Stage: Tritium concentrations at monitoring points in the process room climb rapidly, grow slowly, then approach a constant value. This phenomenon in the glove box is easily understood because all tritium in the room originates from the glove box. The concentration at PR-M2 increases

fastest and remains highest throughout because it is the closest monitoring point to Hole-2. Within an extremely short time (0.05 s) after the accident, tritium concentration exceeds both the alarm setpoint and isolation setpoint. From a safety perspective, PR-M2 should be selected as the reference monitoring point. At the end of the release stage (300 s), process room tritium concentration reaches $1.01 \sim 7.05 \times 10^{14}$ Bq/m^3, after which the DS begins purging.

(2) Tritium Removal Stage: When the DS activates, clean air gradually enters the process room and disrupts the original tritium distribution pattern. Tritium is driven out of the room by purge air, whose volume exceeds that escaping from the glove box through Hole-2, causing concentration to decrease. After a short period (within 30 s) of irregular decline, concentrations at all monitoring points become nearly log-linear graphs. The highest removal rate occurs at PR-M2 because no back-mixing occurs there, while the lowest rate occurs at PR-M15 because the primary flow forms a "spiral flow" that prevents direct movement to the exhaust vent. Approximately 1941 s are required for concentration to decrease to the isolation threshold, and about 2667 s to reach the alarm setpoint. One hour of purging can reduce process room concentration to less than 1/1000 of the alarm setpoint and 1/100 of general tritium air monitor detection limits. After DS shutdown, even if all residual tritium from the glove box entered the room, the effect on room concentration would be negligible.

Furthermore, tritium concentration slices and contours intuitively represent spilled tritium movement in the second and third confinement barriers, aiding explanation of the process and mechanism. The impact of the emergency system on tritium transport was observed, and key times were identified to evaluate the conceptual design of the current tritium removal system against safety requirements.

Only first-stage results have been summarized. Many factors affect tritium transport, including breach size, location, and shape; DS vent location and size; purge gas velocity and direction; and emergency system response time. A more comprehensive and systematic three-dimensional numerical simulation is underway, with results to be reported.

Acknowledgments

This work is supported by the National Key R&D Program of China-National Magnetic Confinement Fusion Science Program (Grant No. 2017YFE0300305). Special thanks to Jinguang Cai and Xianglin Wang from the China Academy of Engineering Physics for providing valuable design information on the CFETR tritium plant.

Author Contributions

All authors contributed to study conception and design. Material preparation, data collection, and analysis were performed by Haixia Wang, Xuewei Fu, Weip-

ing Liu, Taosheng Li, and Jie Yu. The first draft was written by Haixia Wang, and all authors commented on previous versions. All authors read and approved the final manuscript.

References

[1] M. Glugla, A. Antipenkov, S. Beloglazov, et al., The ITER tritium systems. Fusion Eng. Des. 82, 472-287 (2007). doi: 10.1016/j.fusengdes.2007.02.025
[2] Y. N. Hrstensmeyer, B. Butler, C. Day, et al., Analysis of the EU-DEMO fuel cycle elements: Intrinsic impact of technology choices. Fusion Eng. Des. 136, 314-318 (2018). doi: 10.1016/j.fusengdes.2018.02.015
[3] X. L. Wang, G. M. Ran, H. Y. Wang, et al., Current Progress of Tritium Fuel Cycle Technology for CFETR. J. Fusion Energ. 38(1), 125-137(2019). doi: 10.1007/s10894-018-0158-1
[4] X. C. Nie, J. Li, S. L. Liu, et al., Global variance reduction method for global Monte Carlo particle transport simulations of CFETR. Nucl. Sci. Tech., 28(08), 127-133(2017). doi: 10.1007/s41365-017-0270-3
[5] Y. Du, Y. Yang, S. B. Jiang, et al., An autocontrol detritiation system. Nuclear Techniques. 33(03), 233-236. (Chinese, Shanghai, 2010)
[6] T. Hayashi, K. Kobayashi, Y. Iwai, et al., Tritium behavior intentionally released in the radiological controlled room under the US-Japan collaboration at TSTA/LANL. Fusion Technol. 34(3P2), 521-525(1998). doi: 10.13182/FST98-A11963665
[7] T. Hayashi, K. Kobayashi, Y. Iwai, Tritium behavior in the Caisson, a simulated fusion reactor room. Fusion Eng. Des. 51, 543-548(2000). doi: 10.1016/S0920-3796(00)00214-3
[8] Y. Iwai, T. Hayashi, T. Yamanishi, et al., Simulation of Tritium Behavior after Intended Tritium Release in Ventilated Room. J. Nucl. Sci. Technol. 38(1), 63-75(2001). doi: 10.1080/18811248.2001.9715008
[9] Y. Iwai, T. Hayashi , K. Kobayashi, et al., Simulation study of intentional tritium release experiments in the caisson assembly for tritium safety at the TPL/JAERI. Fusion Eng. Des. 54(3-4), 523-535(2001). doi: 10.1016/S0920-3796(00)00581-0
[10] W Li, H.Q Kou, X.G. Zeng, et al., Numerical simulations on the leakage and diffusion of tritium. Fusion Eng. Des. 159: ,111749(2020). doi:10.1016/j.fusengdes.2020.111749
[11] H. M. Sahin, G. Tunc, A. Karakoc, et al., Neutronic study on the effect of first wall material thickness on tritium production and material damage in a fusion reactor. Nucl. Sci. Tech., 33(04), 134-151(2022). doi: 10.1007/s41365-022-01029-7
[12] C. J. Li, X. F. Cai, M. Q. Xiao, et al., Analysis on the influencing factors of radioactive tritium leakage and diffusion from an indoor high-pressure storage vessel. Nucl. Sci. Tech., 33(12), 3-13(2022). doi:10.1007/s41365-022-01147-2
[13] B. Feng, W. H. Zhuo, Levels and behavior of environmental tritium in East Asia. Nucl. Sci. Tech., 33(07), 55-73(2022). doi: 10.1007/s41365-022-01073-3
[14] J.C. Han, H.X. Wang, T.S. Li, et al., Simulation Study of Tritium

Transport in CFETR TEP Glove Box based on COMSOL. Nuclear Safety. 21(5): 72-80. (Chinese, Beijing, 2022) doi: 10.16432/j.cnki.1672-
[15] H.X. Wang, X.W. Fu, J.C. Han, et al., Numerical simulation of tritium behavior in tritium confinement system for China fusion engineering test reactor. Paper presented at the 9th Computational Fluid Dynamics for Nuclear Reactor Safety, Texas A&M University, 20-22 February 2023
[16] D. H. Daher, M. Kotb, A. M. Khalaf, et al., Simulation of a molten salt fast reactor using the COMSOL Multiphysics software. Nucl. Sci. Tech. 31(12), 3-21(2020). doi: 10.1007/s41365-020-00833-3
[17] ITER Organization, Preliminary Safety Report (RPrS). (DAC files, Saint Paul-lez-Durance, 2011)
[18] G. M. Ran, J. G. Cai, H. Y. Wang, et al., The CFETR tritium plant: Requirements and design progress. Fusion Eng. Des. 159, 111930(2020). doi: 10.1016/j.fusengdes.2020.111930
[19] M. Saeed, J. Y. Yu, A. A. A. Abdalla, et al., An assessment of k-turbulence models for gas distribution analysis. Nucl. Sci. Tech. 28(10), 86-93(2017). doi: 10.1007/s41365-017-0304-x
[20] G. Y. Liu, Dissertation, University of South China. (Chinese, Hengyang, 2017)